

Experimental Evidence for Resecretion of PGE₂ across Rat Alveolar Epithelium by OATP2A1/SLCO2A1-Mediated Transcellular Transport^[S]

Takeo Nakanishi, Hiroki Takashima, Yuka Uetoko, Hisakazu Komori, and Ikumi Tamai

Faculty of Pharmaceutical Sciences, Institute of Medical, Pharmaceutical and Health Sciences, Kanazawa University, Kanazawa, Japan

Received April 16, 2018; accepted November 8, 2018

ABSTRACT

Prostaglandin transporter *Oatp2a1/Slco2a1* is expressed at the apical (AP) membranes of type-1 alveolar epithelial (AT1) cells. To investigate the role of OATP2A1 in prostaglandin E₂ (PGE₂) handling by alveolar epithelium, we studied PGE₂ transport across and secretion from monolayers of rat AT1-like (AT1-L) cells obtained by trans-differentiation of type-2 alveolar epithelial cells isolated from male Wistar rats. Rat AT1-L cells expressed *Oatp2a1/Slco2a1*, together with smaller amounts of *Mrp4/Abcc4* and *Oct1/Slc22a1*. PGE₂ uptake was saturable with *K_m* 43.9 ± 21.9 nM. Transcellular transport of PGE₂ across AT1-L cells grown on permeable filters in the AP-to-basolateral (BL) direction was 5-fold greater than that in the reverse direction and was saturable with *K_m* 118 ± 26.8 nM; it was significantly inhibited by OATP inhibitors bromosulphophthalein (BSP) and

suramin, and an MRP4 inhibitor, Ceefourin 1. We simultaneously monitored the effects of BSP on the distribution of PGE₂ produced by bradykinin-treated AT1-L cells and PGE₂-d₄ externally added on the AP side of the cells. In the presence of BSP, PGE₂ increased more rapidly on the AP side, whereas PGE₂-d₄ decreased more slowly on the AP side. The decrease in PGE₂-d₄ from the AP side corresponded well to the increase on the BL side, indicating that intracellular metabolism did not occur. These results suggest that *Oatp2a1* and *Mrp4* mediate trans-epithelial transport of PGE₂ in the AP-to-BL direction. Therefore, OATP2A1 may be an important regulator of PGE₂ in alveolar epithelium by reducing secretion of PGE₂ and facilitating “resecretion” of PGE₂ present in the alveolar lumen to the interstitial space or blood.

Introduction

There is significant evidence that PGE₂ exhibits antifibrotic action in the lungs. In vitro studies suggest that PGE₂ suppresses various metabolic capabilities of fibroblasts, including collagen production and transdifferentiation to myofibroblasts (Kolodnick et al., 2003; Moore et al., 2005; Huang et al., 2007), resulting in increased sensitivity of fibroblasts to apoptosis. Thus, insufficient prostaglandin E₂ (PGE₂) generation has been suggested as a contributor to pulmonary fibrosis (Maher et al., 2010). This notion is supported by evidence that *Cox-2*-deficient mice are more susceptible to bleomycin-induced fibrosis (Keerthisingam et al., 2001; Bonner et al., 2002); however, eicosanoids other than PGE₂ (e.g., PGI₂ and PGF_{2α}) are also claimed to play a role in the progression of pulmonary fibrosis (Lovgren et al., 2006; Oga et al., 2009). PGE₂ is present as an organic anion under physiologic conditions and requires an uptake carrier to be

reimported (Sekine et al., 1997; Schuster, 1998; Tamai et al., 2000; Kimura et al., 2002; Gose et al., 2016). Indeed, OATP2A1 encoded by *SLCO2A1* has been characterized as a high-affinity prostaglandin uptake transporter (Kanai et al., 1995; Chan et al., 1998) and measurements of its intra- and extracellular concentrations indicate that it plays a role in PGE₂ signaling (Chi et al., 2006, 2008; Syeda et al., 2012; Nakanishi et al., 2017).

OATP2A1 is abundantly expressed in the lungs of rodents and humans (Kanai et al., 1995; Lu et al., 1996; Pucci et al., 1999; Chang et al., 2010), especially in endothelial cells, where it mediates rapid clearance of PGE₂ from the systemic circulation through the pulmonary vascular beds (Ferreira and Vane, 1967). We recently found that OATP2A1 is expressed in type 1 alveolar epithelial (AT1) cells in mouse lung, as well as primary-cultured rodent AT1 cell-like (AT1-L) cells, and that pulmonary fibrosis was more severe in intratracheally bleomycin-administered *Slco2a1*-null mice (*Slco2a1*^{−/−}), which show lower and higher concentrations of PGE₂ in lung tissue and alveolar lumen, respectively, compared with *Slco2a1* wild-type mice (*Slco2a1*^{+/+}) (Nakanishi et al., 2015). Thus, our previous results suggest that OATP2A1 regulates the pulmonary distribution of PGE₂ produced by epithelial cells and inflammatory cells in the lumen of alveoli.

This work was supported by the Grant-in-Aid for Scientific Research [KAKENHI 15H04755 to T.N.]; and the Japan Society for the Promotion of Science and the Smoking Research Foundation [Grant 055 to T.N.]. None of the authors declare a conflict of interest.

<https://doi.org/10.1124/jpet.118.249789>

[S] This article has supplemental material available at jpet.aspetjournals.org.

ABBREVIATIONS: AEL, alveolar epithelial lining; ANOVA, analysis of variance; AP, apical; AT1, type 1 alveolar epithelial; AT2, type 2 alveolar epithelial; AT1-L, AT1 cell-like; BL, basolateral; BSP, bromosulphophthalein; HEK, human embryonic kidney; *K_m*, Michaelis-Menten constant; LC-MS/MS, liquid chromatography–tandem mass spectrometry; *P_c*, cellular permeability of PGE₂; PGE₂, prostaglandin E₂; *V_{max}*, maximal rate of uptake.

Nevertheless, it is not fully understood how OATP2A1 is involved in PGE₂ handling by alveolar epithelial cells.

In the present study, alveolar type 2 epithelial (AT2) cells prepared from Wistar rats were transdifferentiated into AT1 cell-like (AT1-L) cells, and the function of OATP2A1 in AT1-L cells was characterized by means of cellular uptake and transcellular transport studies of native PGE₂ and externally applied [³H]PGE₂ and PGE₂-d₄. The effects of an OATP2A1 inhibitor, bromosulphophthalein (BSP), were also examined. Our results suggest a role for OATP2A1 in transcellular transport of PGE₂ across AT1 cells in the direction from the alveolar lumen [apical (AP) side to the interstitial space (basolateral, BL, side)]. Thus, OATP2A1 may mediate the redistribution of secreted PGE₂ in the lumen of alveoli to the interstitial space for reuse.

Materials and Methods

Materials. [5,6,8,11,12,14,15-³H]PGE₂ ([³H]PGE₂; 163.6 Ci/mmol), and unlabeled and deuterium-labeled PGE₂ (PGE₂-d₄) were purchased from PerkinElmer Life Science (Boston, MA) and Cayman Chemical (Ann Arbor, MI), respectively. Bromosulphophthalein, suramin, and Ceefourin 1 were obtained from MilliporeSigma (St. Louis, MO), Tokyo Chemical Industry (Tokyo, Japan), and Abcam (Cambridge, UK), respectively. All other compounds were commercial products of reagent grade from MilliporeSigma, FUJIFILM Wako Pure Chemical Corporation (Osaka, Japan), Thermo Fisher Scientific (Waltham, MA), Kanto Chemical (Tokyo, Japan), and Nacalai Tesque (Kyoto, Japan).

Preparation of AT1-L Cells from Isolated AT2 Cells from Rats. Animal studies were approved by the Committee for the Care and Use of Laboratory Animals of Kanazawa University and conducted in accordance with its guidelines (AP-143148 and -183945). Male Wistar rats (170–210 g body weight, at the age of 7 weeks) were injected intraperitoneally with pentobarbital sodium (50 mg/kg) and given heparin (150 IU; Mochida Pharmaceutical Co., Ltd., Tokyo, Japan) via the jugular vein. AT2 cells were prepared as previously described (Richards et al., 1987; Ikehata et al., 2008). A cannula was made in the trachea after tracheotomy, and the postcaval vein was cut. Subsequently, the lungs were perfused with solution I (136.9 mM NaCl, 8.1 mM Na₂HPO₄, 1.5 mM KH₂PO₄, 2.7 mM KCl, 0.2 mM EDTA-2Na, 0.2 mM EGTA, pH 7.2) through the right ventricle and excised, and the bronchia and alveoli were rinsed several times to remove contaminating inflammatory cells. The lungs were filled with solution III (RPMI1640 medium obtained from FUJIFILM Wako Pure Chemical Corporation, containing 25 mM HEPES and 24 mM NaHCO₃), and then placed in physiologic saline. Solution III containing trypsin (0.25%) was allowed to flow continuously from the cannula into the lungs for 30 minutes at 37°C. The trachea, bronchi, and large airways were removed, and the lung tissues were minced into small pieces and then treated with solution III containing DNase I (250 μg/ml) and tylosin (120 μg/ml). The resultant tissue and cell suspension were filtered through sterile gauze, and nylon net filters of 70-μm (Corning, Corning, NY) and 15-μm (Tanaka Sanjiro, Fukuoka, Japan) pore size. The filtered cell suspension was overlaid on high-density (1.089 g/ml) and low-density (1.040 g/ml) Percoll solutions as previously described (Ikehata et al., 2008), and AT2 cells were obtained by centrifugation at 250g and 4°C for 20 minutes. The cells were resuspended in solution I, and stained with Trypan blue to confirm viability. AT2 cells from preparations with a viability of over 90% were cultured for 6 days in Dulbecco's modified Eagle's medium (DMEM) supplemented with 10% fetal bovine serum (FUJIFILM Wako Pure Chemical Corporation) at 37°C under an atmosphere of 5% CO₂ in air.

PGE₂ Uptake by Rat AT1-L Cells and Human Embryonic Kidney 2A1 Cells Expressing Human OATP2A1. For apical

uptake studies, AT2 cells were seeded on multiple tissue culture plates (2 × 10⁵ cells/cm²) for 6 days, and then used for [³H]PGE₂ uptake in the absence or presence of an OATP inhibitor as described before (Nakanishi et al., 2015). Human embryonic kidney (HEK)293 cells transfected with *SLCO2A1* gene (HEK/2A1) were prepared for uptake assay as described previously (Gose et al., 2016). Intracellular accumulation of [³H]PGE₂ was evaluated by measuring radioactivity in cell lysates with a liquid scintillation counter (Hitachi Aloka Medical, Tokyo, Japan); results are shown as cell-to-medium ratio normalized by protein content (microliter per milligram protein). The Michaelis constant (*K_m*) and the maximal rate of uptake (*V_{max}*) were obtained by fitting the data to the following equation,

$$v = \frac{V_{max} \times S}{K_m + S} \quad (1)$$

where *v* and *S* are the uptake rate and the initial concentration of PGE₂, respectively. Kinetic parameters *K_m* and *V_{max}* were estimated by means of nonlinear least-squares analysis using KaleidaGraph (ver. 4.0J; HULINKS, Tokyo, Japan).

PGE₂ Transcellular Transport across and Secretion from Rat AT1-L Cells. AT1-L cells were plated on fibronectin (1 μg/well; MilliporeSigma) -coated Transwell filter membrane inserts with a 0.4-μm pore size and 6.5-mm diameter (Becton Dickinson, Franklin Lakes, NJ) at a density of 2.0 × 10⁵ cells/well for 6 days. The cells were preincubated for 15 minutes at 37°C with transport medium (4.8 mM KCl, 125 mM NaCl, 1.2 mM KH₂PO₄, 1.2 mM CaCl₂, 1.2 mM MgSO₄, 5.6 mM glucose, 25 mM HEPES, pH 7.4, adjusted with NaOH). Basically, cells grown on filters with transepithelial electrical resistance of 500 (Ω·cm²) or more were used for transport study. Transport was initiated by adding transport medium containing [³H]PGE₂ (2.78 nM; e.g., 0.5 μCi/ml) or deuterium-labeled PGE₂ (PGE₂-d₄) and/or [¹⁴C]mannitol (0.5 μCi/ml) to the AP (250 μl) or BL (1000 μl) side in the presence or absence of an inhibitor of the transporter of interest on both sides. To analyze PGE₂ secretion, endogenous PGE₂ was measured in DMEM without fetal bovine serum on both sides of cells treated with bradykinin (10 μM), which is an inducer of prostaglandin synthesis. At the designated time, transport medium was withdrawn for measurement from the AP (10 μl) and BL (100 μl) sides, and supplemented with an equal volume of medium with the same composition, except for PGE₂. At the end of assay, the filter membrane was washed with ice-cold transport medium and the cells were collected to measure the intracellular content of substrate. Radioactivity in the samples was quantified with a liquid scintillation counter (Hitachi Aloka Medical). Unlabeled or deuterium-labeled PGE₂ was quantified with LC-MS/MS as described below. The apparent permeability of PGE₂ across the cell monolayer was calculated as permeability coefficient (*P_c*, cm/s) using the following equation,

$$P_c = \frac{\left(\frac{dQ}{dt}\right)}{A \times S} \quad (2)$$

where *Q*, *S* and *A* are the amount of PGE₂ over a period of time *t*, the surface area of the filter membrane, and the initial concentration on the donor side, respectively.

PGE₂ Measurements in the Culture Media and Cell Lysate. PGE₂ and PGE₂-d₄ were extracted from culture media and cell lysate into ethyl acetate containing formic acid (v/v, 0.24%) under acidic conditions; PGF_{2α}-d₄ was used as an internal standard. The combined organic phase was dried under reduced pressure, reconstituted with acetonitrile containing 0.1% formic acid for analysis, and subjected to liquid chromatography–tandem mass spectrometry (LC-MS/MS) using an LCMS8050 triple quadrupole mass spectrometer (Shimadzu Co., Kyoto, Japan) coupled with an LC-30AD ultra-fast liquid chromatography system (Shimadzu Co.). The flow rate of the mobile phase was 0.3 ml/min and the injection volume was set as 30 μl. Luna (C18, 20 × 4.0 mm, 3 μm; Phenomenex, Torrance, CA) was used as an analytical column. Samples were kept at 4°C during the

analysis. Electrospray negative ionization was used, and the mass transitions were monitored at m/z 351.00/271.35 for PGE₂, m/z 355.1/319.25 for PGE₂-d₄ and m/z 357.10/313.25 for d₄-PGF_{2 α} . Analyst software Laboratory Solution LCMS was used for data manipulation.

Reverse Transcription-Polymerase Chain Reaction. Total RNA was extracted from AT1-L cells using RNAiso Plus (Takara Bio, Tokyo, Japan) and then reverse-transcribed to cDNA with Moloney murine leukemia virus reverse transcriptase (Promega, Madison, WI). mRNA expression of 11 rat transporter genes was evaluated with the respective sequence primers (listed in Supplemental Table 1). Polymerase chain reaction products were visualized on 1.5% agarose gel with ethidium bromide.

Western Blotting. Western blot analysis was performed as described previously (Shimada et al., 2015). The cells were homogenized by sonication (Qsonica, LLC., Newtown, CT) and lysed in RIPA buffer (150 mM sodium chloride, 1% Nonidet P (NP)-40, 0.5% sodium deoxycholate, 0.1% SDS, and 50 mM Tris at pH 8.0) containing protease inhibitor cocktail (Nacalai Tesque). For Oatp2a1 and Mrp4, cells were lysed with M-PER buffer (Life Technologies/Thermo Fisher Scientific, Carlsbad, CA). Lysates were separated from nuclei and unbroken cells by centrifugation (10,000g), at 4°C for 10 minutes, and protein concentration was determined using a Bio-Rad protein assay kit (Hercules, CA). A 20- to 40- μ g aliquot of the total cell lysate was separated in SDS polyacrylamide gel (8% or 10%) and then electrotransferred onto a polyvinylidene difluoride membrane (Merck Millipore, Burlington, MA). The membranes were treated with 5% nonfat dry milk in TBS-T (0.1% Tween 20-containing Tris-buffered saline) to block nonspecific binding for 1 hour at room temperature, and then incubated overnight at 4°C with antibody diluted in 5% nonfat dry milk in TBS-T using primary antibodies against Cox-2, 15-Pgdh (1:250 dilution; Cayman Chemical), and Gapdh (1:5000 dilution; Cell Signaling Technology, Danvers, MA). Anti-Oatp2a1 (1:1000 dilution; Atlas Antibodies, Stockholm, Sweden) and anti-Mrp4 (1:1000 dilution; Vector Laboratories, Burlingame, CA) antibodies were used with Immobilon signal enhancer (Merck Millipore). The membrane was treated with horseradish peroxidase (HRP)-conjugated anti-rabbit secondary antibody (1:2000 to 1:5000 dilution; Life Technologies) for 1 hour at room temperature, and bands were revealed with ImmunoStar Zeta (FUJIFILM Wako Pure Chemical Corporation). For Mrp4, the membranes incubated with primary antibody were reacted with biotin-conjugated goat anti-rabbit IgG (1:2000; Vector Laboratories) for 2 hours at room temperature, and then treated with HRP-conjugated streptavidin (1:2000; Thermo Fisher Scientific) for 1 hour at room temperature. The signal was developed as described above. Bands of interest on the blots were analyzed using a CS analyzer (ATTO, Tokyo, Japan).

Statistical Analysis. The statistical significance of differences was analyzed by means of Student's *t* test or one-way analysis of variance (ANOVA) with Bonferroni's multiple comparison test. Multiple comparison was performed with Excel Toukei ver 2.03 software (Social Survey Research Information Co., Ltd., Tokyo, Japan). A *P*-value < 0.05 was considered significant.

Results

Expression of Functional OATP2A1 in Rat AT1-L Cells. mRNA expression levels of 11 genes encoding transporters that recognize prostaglandins as substrates were examined in AT1-L cells by means of reverse transcription-polymerase chain reaction (Fig. 1). mRNA expression of Oatp2a1 was almost exclusively found in AT1-L cells, and Oct1 and Mrp4 were faintly expressed. Oatp2a1 is highly and moderately expressed in rat lung and kidney, respectively (Kanai et al., 1995) but is vice versa for the expression of Mrp4 (Chen and Klaassen, 2004). Protein

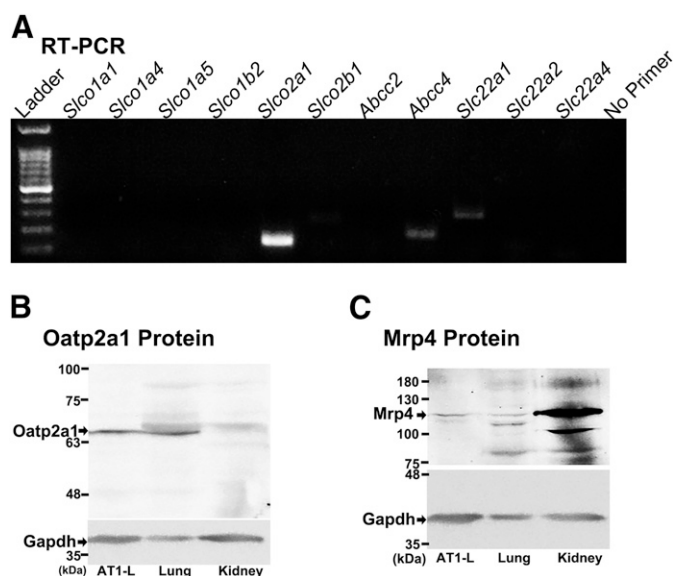


Fig. 1. Expression of transporter genes in rat AT1-L cells. (A) PCR was repeated three times with three independently cultured lots of AT1-L cells. Bands were visualized with ethidium bromide after electrophoresis on 1.5% agarose gel. Primers used are listed in Supplemental Table 1. (B and C) Western blotting was performed for Oatp2a1 (B) and Mrp4 (C) in rat AT1-L cells. Rat lung and kidney homogenates were used as positive controls for Oatp2a1 and Mrp4, respectively. Experiments were repeated three times with two separately prepared lots of AT1-L cells, and representative Western blots are shown.

expression of Oatp2a1 and Mrp4 in AT1-L cells was assessed by Western blot analysis with homogenates of rat lung and kidney. The blots showed specific bands corresponding to Oatp2a1 (65 kDa) and Mrp4 (120 kDa) in AT1-L cells as detected in lung and kidney, respectively (Fig. 1, B and C). Initial apical uptake of PGE₂ (determined at 2 minutes) by AT1-L cells grown on plates was saturable, and *K_m* and *V_{max}* were estimated as 43.9 ± 21.9 nM and 0.77 pmol/2 min per milligram protein, respectively (Fig. 2A). An Eadie-Hofstee plot (inset of Fig. 2A) revealed a single saturable component. Apical uptake of [³H]PGE₂ was significantly decreased in the presence of unlabeled PGE₂, a pan-OATP inhibitor BSP, or a selective OATP2A1 inhibitor TGBz 34A (TGBz) at 25 μ M (Chi et al., 2006), and no significant difference was detected among the uptakes in the presence of these three inhibitors (Fig. 2B, one-way ANOVA with Bonferroni's multiple comparisons test, *P*-value > 0.05). Thus, since the inhibitory potential of BSP on PGE₂ uptake was comparable to that of TGBz in AT1-L cells, BSP was used as an OATP2A1 inhibitor in the following experiments.

Transcellular Transport of PGE₂ across AT1-L Cells. The AP-to-BL and BL-to-AP permeability of [³H]PGE₂ was measured in rat AT1-L cells cultured on permeable filters. Figure 3A shows time course of transcellular transport of [³H]PGE₂ in the AP-to-BL direction. Permeated radioactivity on the BL side increased linearly for 40 minutes, and was significantly reduced by 73.0% in the presence of BSP, which is similar to the effect on initial uptake of PGE₂ from the AP side. The cellular permeability values of PGE₂ AP-to-BL transport (*P_{cA→B}*) were calculated as 4.27 and 0.83×10^{-5} cm/s in the absence (control) and in the presence of BSP, respectively (Fig. 3B), whereas *P_{cA→B}* of mannitol, a marker for paracellular transport, corresponded to only 4.0% of the

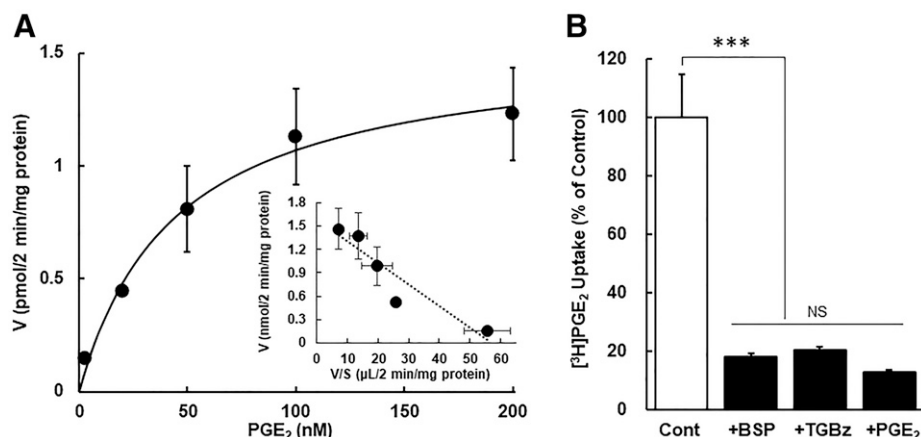


Fig. 2. PGE₂ uptake by AT1-L cells. (A) Saturation kinetics of PGE₂ uptake by AT1-L cells was analyzed according to the Michaelis-Menten equation. Experiments were repeated multiple times, and each point represents the mean value \pm S.E.M. of three separate cell lots. The inset shows an Eadie-Hofstee plot of the data. (B) PGE₂ uptake by AT1-L was evaluated in the absence (Cont) or presence of BSP, TGBz, or unlabeled PGE₂ at 25 μ M. Each bar represents the mean value of three individual cell lots with S.E.M. Statistical analysis was conducted by one-way ANOVA with Bonferroni's multiple comparisons test: *** P < 0.001. NS, no significant difference.

control $P_{c,A \rightarrow B}$ of PGE₂, and was not affected by BSP. The P_c in the reverse direction ($P_{c,B \rightarrow A}$) of PGE₂ (0.71×10^{-5} cm/s) was almost five times lower than its $P_{c,A \rightarrow B}$ (4.27×10^{-5} cm/s) but was still higher than $P_{c,B \rightarrow A}$ of mannitol (0.27×10^{-5} cm/s). Because $P_{c,B \rightarrow A}$ of PGE₂ was not reduced by BSP, the contribution of OATP2A1 to BL-to-AP transport of PGE₂ appears to be negligible (Fig. 3B). The AP-to-BL transport of PGE₂ was saturable with a K_m of 118 ± 26.8 nM (Fig. 3C). Moreover, $P_{c,A \rightarrow B}$ of PGE₂ was significantly reduced in the presence of TGBz or suramin, which was used as a more selective inhibitor of OATP2A1 (Kamo et al., 2017). $P_{c,A \rightarrow B}$ of PGE₂ measured in the presence of a pan-inhibitor of OCTs, tetraethylammonium (TEA), was significantly higher than that with TGBz or suramin but was not different from that in the absence of inhibitor (Fig. 3D, one-way ANOVA with Bonferroni's multiple comparisons). Furthermore, PGE₂ is exported by MRP4 (Reid et al., 2003); therefore, we further examined the effect of Ceefourin 1, a specific inhibitor of MRP4 (Cheung et al., 2014), on transcellular PGE₂ transport. The $P_{c,A \rightarrow B}$ of PGE₂ was somewhat reduced by Ceefourin 1 (Fig. 4A), but increasing concentrations of Ceefourin 1 did not cause any statistically significant changes of OATP2A1-mediated PGE₂ uptake in HEK/2A1 cells (Fig. 4B, one-way ANOVA with Bonferroni's multiple comparisons test, P -value > 0.05). These results suggest that MRP4 may make only a minor contribution to PGE₂ efflux at the BL membranes of AT1-L cells.

Impact of OATP2A1 Inhibitor on PGE₂ Disposition in Rat AT1-L Cells. We explored further the role of OATP2A1 in PGE₂ handling by alveolar epithelium, where secretion, reuptake, transcellular transport, and metabolism of PGE₂, synthesized by not only alveolar epithelial cells but also other type of cells, all occur simultaneously. First, expression of rate-limiting enzymes of PGE₂ synthesis and metabolism was examined in rat AT1-L cells. Western blot analysis showed constitutive expression of Cox-2 and 15-Pgdh in AT1-L cells at significant levels (Fig. 5). Indeed, 15-ketoPGE₂, which is a metabolite of PGE₂ produced by 15-PGDH, was found in AT1-L cells grown on filters when they were treated with an inflammatory mediator, bradykinin, to induce PGE₂ synthesis. Furthermore, to mimic the disposition of PGE₂ produced by cells other than AT1 cells in alveolar epithelial lining (AEL) fluid, PGE₂-d₄ (20 nM) was externally added on the AP side of bradykinin-treated AT1-L cells, and the effects of BSP on the distributions of PGE₂-d₄ and endogenous PGE₂

were simultaneously monitored for 4 hours. On the AP side, accumulation of endogenous PGE₂ increased in a time-dependent manner. In the presence of BSP, accumulation of PGE₂ was further increased after 1 hour, and cumulative PGE₂ was significantly larger from 2 to 4 hours than that in the absence of BSP (Fig. 6A). BSP elevated the rate of increase in endogenous PGE₂ on the AP side from 0.041 to 0.061 pmol/h (1.5-fold), compared with that in control cells (Table 1). The rate of decrease of applied PGE₂-d₄ on the AP side of control cells (0.577 pmol/h) was significantly slowed to 0.397 pmol/h by BSP (Table 1), and consequently the remaining amount of PGE₂-d₄ at 4 hours was increased from 49.3% to 71.3% of the initially applied amount (Fig. 6B). The intracellular amount of PGE₂ in BSP-treated cells (0.220 pmol/filter) was significantly lower than that in control cells at 4 hours (0.263 pmol/filter, Table 2). The amounts in BSP-treated and control cells accounted for 17.3% and 21.8% of the sum of PGE₂ and 15-ketoPGE₂ detected at 4 hours, respectively. On the other hand, the amounts of both PGE₂ and PGE₂-d₄ on the BL side increased in a time-dependent manner (Fig. 6, C and D), whereas PGE₂ accumulation on the BL side was not affected by BSP (Fig. 6C). The average appearance rate of PGE₂-d₄ on the BL side was significantly decreased in the presence of BSP from 0.627 to 0.412 pmol/h at 4 hours (Fig. 6D; Table 1). Regardless of the presence of BSP, the increase in PGE₂-d₄ on the BL side was almost equal to its decrease on the AP side: PGE₂-d₄ decreased by 2.31 ± 0.11 and 1.59 ± 0.25 (pmol) on the AP side of untreated and BSP-treated cells, whereas it increased by 2.53 ± 0.03 and 1.61 ± 0.13 (pmol) in BL side, respectively. The intracellular amounts of PGE₂-d₄ in the absence and presence of BSP were 0.015 and 0.019 pmol/filter (Table 2), which accounted for 0.33% and 0.35% of the initial dose, respectively; these are not significantly different. The proportions of remaining PGE₂-d₄ in AT1-L cells were much lower than those of PGE₂, regardless of the presence of BSP (Table 2), implying a difference in intracellular compartmentalization of endogenous and exogenous PGE₂. 15-Keto PGE₂ was detected at similar levels in both control and BSP-treated cells; however, the deuterium-labeled metabolite was not detected in the cells or the extracellular medium (Tables 1 and 2).

Discussion

Our present findings demonstrate that PGE₂ is transported by OATP2A1 across monolayers of primary-cultured rat

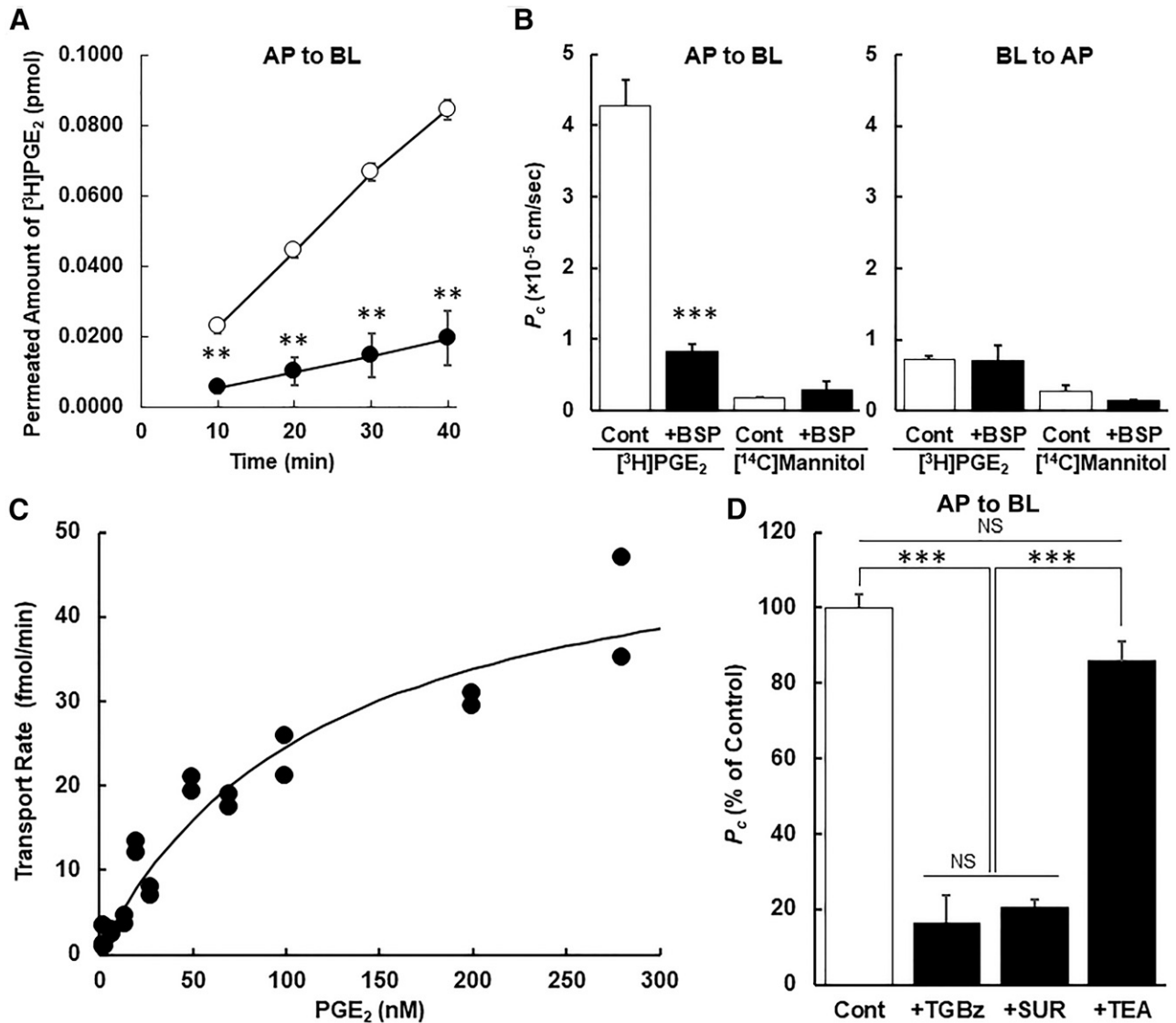


Fig. 3. Characterization of PGE₂ transport across monolayers of AT1-L cells. (A) Transport of [³H]PGE₂ (2.78 nM) was monitored in the short term. Open and closed symbols indicate cumulative amounts of [³H]PGE₂ in the absence and the presence of 25 μ M BSP. Experiments were repeated at least three times, and each point represents the mean of three results from separate cell lots with S.E.M. Statistical analysis was conducted with Student's *t* test; ***P* < 0.01. (B) Effect of BSP on P_c of PGE₂ and mannitol. P_c was evaluated for transcellular transport of [³H]PGE₂ and [¹⁴C]mannitol in the absence (Cont) or in the presence of BSP (25 μ M). Each bar represents the mean of three results from separate cell lots with S.E.M. Statistical analysis was conducted with Student's *t* test; ****P* < 0.001. (C) Saturation kinetics of AP-to-BL transport of PGE₂. Experiments were repeated three times and all data were plotted and analyzed according to the Michaelis-Menten equation. (D) Effects of various compounds on $P_{cA \rightarrow B}$ of PGE₂. The values were obtained in the absence (Cont) or in the presence of TGBz and/or suramin (25 μ M), or tetraethylammonium (100 μ M). Each bar represents the mean of three results from separate cell lots with S.E.M. One-way ANOVA with Bonferroni's multiple comparisons test was used: *** *P* < 0.001. NS, no significant difference.

AT1-L cells grown on permeable filters, suggesting a contribution of OATP2A1 to PGE₂ transport from the AP to BL side of alveolar epithelium. This indicates that PGE₂ secreted to the AEL fluid in alveolar lumen (corresponding to the AP side of AT1 cells) could be reused in the interstitial tissues (BL side) after vectorial transport mediated by OATP2A1 at the AP membrane in conjunction with BL MRP4. Therefore, OATP2A1 could be an important regulator of PGE₂ concentration not only in the AEL fluid but also in the alveolar interstitial spaces.

We previously reported cell-surface expression of Oatp2a1 in rat as well as mouse AT1-L cells (Nakanishi et al., 2015). We also detected robust expression of Oatp2a1 at the mRNA

(Fig. 1A) and protein (Fig. 1B) levels in rat AT1-L cells used in the present study. Although AT1-L cells displayed a single, distinct immunoreactive band for Oatp2a1, the rat lung tissue lysates showed additional bands of molecular sizes greater than 65 kDa. Such immunoreactive bands were also observed in the rat kidney lysates expressing a low level of Oatp2a1 and may represent more matured forms of Oatp2a1 by post-translational modifications. The specific band observed in AT1-L cells and lung is thought to represent de novo-synthesized Oatp2a1. Furthermore, the K_m value for PGE₂ uptake by rat AT1-L cells was estimated as 43.9 nM (Fig. 2A), which is similar to the reported K_m value of PGE₂ uptake by rat Oatp2a1 (Kanai et al., 1995), and the effects of Oatp2a1

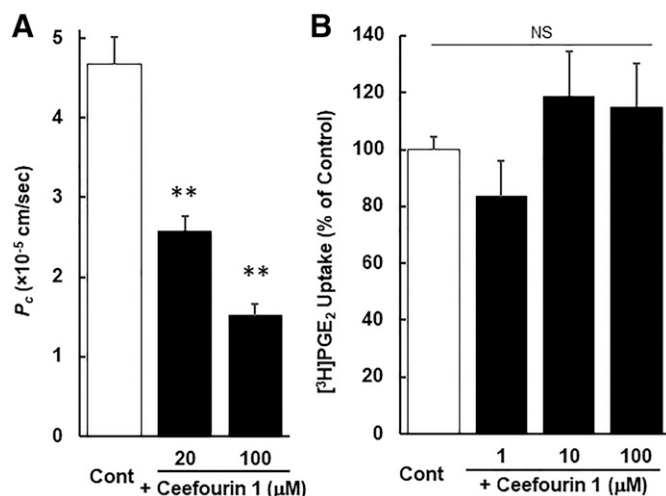


Fig. 4. Characterization of PGE_2 transport across monolayers of AT1-L cells. (A) Effect of Ceefourin 1 on P_c of PGE_2 . P_c was evaluated in transcellular transport of $[^3H]PGE_2$ in the absence (Cont) or the presence of Ceefourin 1 at the indicated concentration. Each bar represents the mean of three results from individual cell lots with S.E.M. Statistical analysis was conducted with Student's t test: ** $P < 0.01$. (B) Effect of Ceefourin 1 on PGE_2 uptake by HEK/2A1 cells overexpressing human OATP2A1. Statistical analysis was conducted by one-way ANOVA with Bonferroni's multiple comparisons test. NS, no significant difference.

inhibition were consistent with our previous findings (Nakanishi et al., 2015). Therefore, AT1-L cells are considered to be a reasonable experimental model to evaluate Oatp2a1 function at the alveolar epithelium. Transcellular PGE_2 transport across monolayers of rat AT1-L cells was further investigated in the present study. Apparent transcellular transport of PGE_2 was observed from the AP to the BL side but was small in the reverse direction, indicating that PGE_2 uptake from the BL side is small (Fig. 3, A and B). Thus, Oatp2a1 may function at the apical membranes of AT1-L cells. $P_{c,A \rightarrow B}$ of PGE_2 was significantly decreased in the presence of various OATP2A1 inhibitors but not organic cation transporter inhibitor TEA (Fig. 3, B and D). The K_m for AP-to-BL transport of PGE_2 (118 nM) was 2.7-fold greater than that for PGE_2 uptake by rat AT1-L cells (Fig. 2A), but it was close to the reported K_m for rat Oatp2a1 (94 nM) (Kanai et al., 1995). Considering the marginal PGE_2 uptake by rat AT2 cells and Oatp2a1 expression in AT1 cells of mouse lung (Nakanishi et al., 2015), our current results suggest that apically expressed OATP2A1 could be the predominant contributor to transepithelial transport of PGE_2 in rat AT1 cells. We also observed protein expression of Mrp4 in AT1-L cells (Fig. 1C) and partial inhibition of PGE_2 transport by Ceefourin 1 (Fig. 4A). Previous literature indicates that no specialized transporter is required for efflux process at the BL membranes (Nomura et al., 2004); however, MRP4 may contribute to cellular efflux in AT1 cells. Although we could not determine the subcellular localization of Mrp4 in rat AT1-L cells, immunoreactivity of Mrp4 has been observed in intracellular spaces of human alveolar epithelial cells (Torky et al., 2005; van der Deen et al., 2005). Further study is needed to establish in detail the mechanism of PGE_2 export in alveolar epithelium.

PGE_2 disposition in AEL fluid is mediated by different types of cell, including alveolar epithelial cells, inflammatory cells, such as alveolar macrophages, and some interstitial cells,

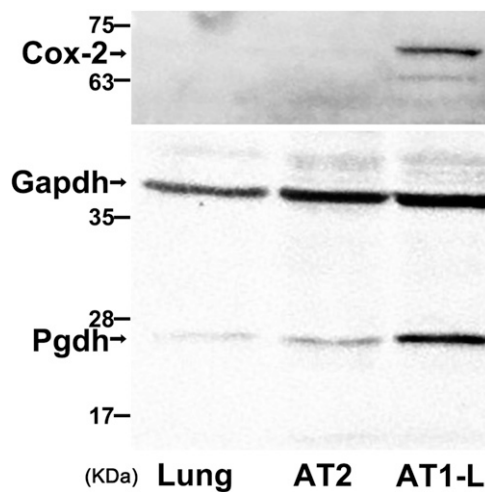


Fig. 5. Western blot for Cox-2 and 15-Pgdh in rat AT1-L cells. Western blotting was performed for Cox-2 and Pgdh in rat lung and primary cultured alveolar epithelial cells. Experiments were repeated three times with separately prepared lots of AT1-L cells. Representative Western blots are shown.

because they all can also produce PGE_2 under inflammatory conditions. The alveolar surface is mostly covered with AT1 cells, so OATP2A1 may have a significant role in PGE_2 disposition in the respiratory regions. Hence, in the present study, the role of Oatp2a1 in PGE_2 handling by alveolar epithelium was examined in bradykinin-treated rat AT1-L cells constitutively expressing Cox-2 and 15-Pgdh (Fig. 5). Externally added PGE_2 -d₄ on the AP side mimics secreted or accumulated PGE_2 in the AEL fluid. Since the physiologically relevant PGE_2 concentration in AEL fluid is unknown, the PGE_2 -d₄ concentration was set at 20 nM, because the dissociation constant of PGE_2 for rat EP receptors is in the range of 1 (to EP4) to 24 nM (to EP1) (Boie et al., 1997; Dey et al., 2006). Our transport study of PGE_2 across monolayers of rat AT1-L cells showed: 1) a BSP-induced increase in AP PGE_2 concentration (Fig. 6, A and B), 2) consistent transport of PGE_2 -d₄ in the AP-to-BL direction (Fig. 6, B and D), and 3) predominant secretion of PGE_2 toward the BL side (Fig. 6, A and C). Given the dominant role of Oatp2a1 in PGE_2 uptake from the AP side of AT1-L cells, impaired function of OATP2A1 may result in an increase in PGE_2 concentration in the AEL fluid owing to elevated PGE_2 secretion, reflecting reduced reuptake and decreased transport of pooled/secreted PGE_2 in AEL. This observation agrees well with a report of elevated PGE_2 level in BAL of bleomycin-administered *Sclo2a1*^{-/-} mice (Nakanishi et al., 2015).

Our study also showed that PGE_2 on the AP side of cells could be transported to the BL side without being metabolized, because the increase in the remaining amount of exogenous PGE_2 in the presence of BSP was counterbalanced by the decrease in its amount on the BL side. Indeed, much less PGE_2 -d₄ (approximately 0.3%) than PGE_2 (17.5%–21.7%) remained in cells, and no metabolite of PGE_2 -d₄ was found in either cells or extracellular medium (Table 1), although 15-Pgdh expression was observed in AT1-L cells (Fig. 5) and 15-keto PGE_2 was collected from the cells (Table 2). This observation clearly suggests that the distribution of exogenous PGE_2 is distinct from that of newly synthesized PGE_2 , and this can be explained by much faster transfer of exogenous

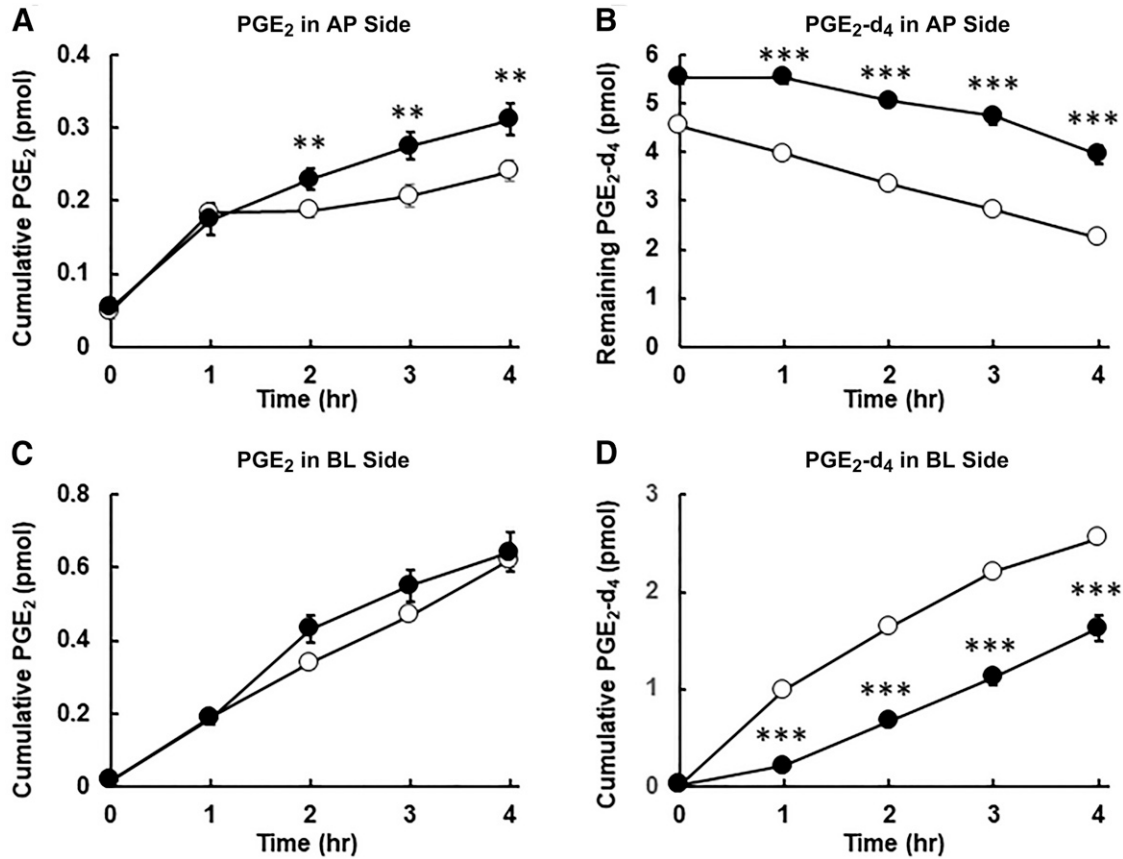


Fig. 6. Effect of BSP on PGE₂ and PGE₂-d₄ disposition. Effect of BSP on accumulation of endogenous PGE₂ (A) and remaining PGE₂-d₄ (B) on the AP side and on accumulation of PGE₂ (C) and PGE₂-d₄ (D) in cells with (closed circles) and without (open circles) BSP. Each point represents the mean of results from six separate cell lots with S.E.M. Statistical analysis was conducted with Student's *t* test: ** and *** indicate *P* < 0.01 and < 0.001, respectively.

PGE₂ across the cell monolayer compared with the rate of metabolism by intracellular 15-Pgdh. Thus, trans-epithelial transport of secreted PGE₂ in alveolar lumen can be regarded as “resecretion” toward the BL side of the cells, to which Oatp2a1 and Mrp4 both contribute. This idea is illustrated in Fig. 7, although the subcellular localization of Mrp4 still needs to be verified. This could provide a route for rapid transfer of PGE₂ into interstitial tissues in the lung. This would be consistent with the reported transport of PGE₂ in Madin-Darby canine kidney cells transfected with hSLCO2A1 (Nomura et al., 2004) and murine collecting duct cells in the kidney (Chi et al., 2008). Our present study is the first demonstration of this concept in primary-cultured cells. It is noteworthy that the cumulative amount of PGE₂ at 4 hours on

the BL side (0.62 ± 0.02 pmol) was approximately 2.6 times higher than that on the AP side (0.24 ± 0.02 pmol) in control cells (Fig. 6C), implying polarized secretion of PGE₂ from cells. Our results showed that BSP increased the AP accumulation of PGE₂ (produced by AT1-L cells) by 0.07 pmol (Fig. 6A); however, the difference did not simply reflect the reduction of PGE₂ accumulation on the BL side (Fig. 6C), in contrast to the case of PGE₂-d₄ (Fig. 6, B and D). Further study is needed to establish how intracellularly synthesized PGE₂ is handled by cells.

We previously showed that *Slco2a1*^{-/-} mice administered bleomycin intratracheally exhibit more severe pulmonary fibrosis than wild-type counterparts. Aggravated fibrosis in

TABLE 1

Rates of change of PGE₂ and PGE₂-d₄ in the presence and absence of BSP

Samples were collected from extracellular medium containing 10 μM bradykinin. Metabolites of PGE₂ and PGE₂-d₄ were not detected in extracellular medium. Results show the mean value ± S.E.M. of six wells. Statistical analysis was conducted with Student's *t* test compared with control: *, **, and *** indicate *P* < 0.05, 0.01, and 0.001, respectively.

	AP Side ^a		BL Side	
	Control	+BSP	Control	+BSP
	pmol/h per filter	pmol/h per filter	pmol/h per filter	pmol/h per filter
PGE ₂	0.041 ± 0.003	0.061 ± 0.004**	0.148 ± 0.005	0.161 ± 0.014
PGE ₂ -d ₄	-0.577 ± 0.032	-0.397 ± 0.052*	0.627 ± 0.011	0.412 ± 0.032***

^aA minus sign indicates rate of decrease of PGE₂ or PGE₂-d₄.

TABLE 2

Intracellular accumulation of PGE₂ and its metabolite 15-ketoPGE₂

Results show the mean value ± S.E.M. of six wells. Statistical analysis was conducted with Student's *t* test compared with control: * and ** indicate *P* < 0.05 and 0.01, respectively.

	Control				+BSP			
	Intact	% ^a	Metabolite ^b	% ^a	Intact	% ^a	Metabolite ^b	% ^a
	pmol		pmol		pmol		pmol	
PGE ₂	0.263 ± 0.009	21.7 ± 0.77	0.088 ± 0.004	7.3 ± 0.47	0.220 ± 0.007**	17.3 ± 0.58**	0.107 ± 0.006*	8.50 ± 0.59
PGE ₂ -d ₄	0.015 ± 0.005	0.33 ± 0.10	N.D.	N.D.	0.019 ± 0.002	0.35 ± 0.20	N.D.	N.D.

N.D., not detected.
^aProportions of PGE₂ and PGE₂-d₄ were calculated on the basis of the sum of PGE₂ and 15-ketoPGE₂ at 4 hours (1.21 pmol for control cells and 1.26 pmol for BSP-treated AT1-L cells) and the initial dose of PGE₂-d₄ (4.55 pmol for control cells and 5.54 for BSP-treated cells), as determined by LC-MS/MS.
^bThe only metabolite detected was 15-ketoPGE₂.

Slco2a1^{-/-} mice was associated with an elevated level of PGE₂ in bronchoalveolar lavage fluid and increased phosphorylation of profibrotic protein kinase C (PKC)-δ in the lung tissue (Nakanishi et al., 2015). Previous research has suggested that extracellular PGE₂ suppresses PKC-δ activation, which contributes to collagen production in lung fibroblasts (Huang et al., 2008). On the basis of our present findings, OATP2A1-mediated PGE₂ transport to the interstitial space from AEL fluid may contribute to modulation of PKC-δ activity in fibroblasts. Taken together, these results may provide a new rationale for the enhanced PKC-δ activity in aggravated fibrosis of *Slco2a1*^{-/-} mice.

In conclusion, our study demonstrates that apically expressed OATP2A1 contributes to transcellular transport of PGE₂ across monolayers of rat AT1-L cells. OATP2A1 apparently reduces secretion of endogenous PGE₂ on the AP side and facilitates “resecretion” of exogenous PGE₂ on the BL side of AT1-L cells. This may be an important mechanism for

transferring existing PGE₂ from AEL fluid to interstitial space or blood, thereby contributing not only to efficient elimination of PGE₂ from alveolar lumen but also to the modulation of PGE₂ signaling of interstitial cells such as fibroblasts. A detailed understanding of this role of OATP2A1 in the progression of interstitial pneumonia may provide a clue for developing new therapeutic strategies for pulmonary fibrosis.

Acknowledgments

We thank Sakiyama and Dr. Gose for their technical assistance.

Authorship Contributions

Participated in research design: Nakanishi, Takashima, Tamai.
Conducted experiments: Nakanishi, Takashima, Uetoko, Komori.
Contributed new reagents or analytic tools: Nakanishi, Takashima, Uetoko.
Performed data analysis: Nakanishi, Takashima, Uetoko, Komori.
Wrote or contributed to the writing of the manuscript: Nakanishi, Komori, Tamai.

References

Boie Y, Stocco R, Sawyer N, Slipetz DM, Ungrin MD, Neuschäfer-Rube F, Püschel GP, Metters KM, and Abramovitz M (1997) Molecular cloning and characterization of the four rat prostaglandin E2 prostanoid receptor subtypes. *Eur J Pharmacol* **340**:227–241.
Bonner JC, Rice AB, Ingram JL, Moomaw CR, Nyska A, Bradbury A, Sessoms AR, Chulada PC, Morgan DL, Zeldin DC, et al. (2002) Susceptibility of cyclooxygenase-2-deficient mice to pulmonary fibrogenesis. *Am J Pathol* **161**:459–470.
Chan BS, Satriano JA, Pucci M, and Schuster VL (1998) Mechanism of prostaglandin E2 transport across the plasma membrane of HeLa cells and *Xenopus* oocytes expressing the prostaglandin transporter “PGT”. *J Biol Chem* **273**:6689–6697.
Chang HY, Locker J, Lu R, and Schuster VL (2010) Failure of postnatal ductus arteriosus closure in prostaglandin transporter-deficient mice. *Circulation* **121**:529–536.
Chen C and Klaassen CD (2004) Rat multidrug resistance protein 4 (Mrp4, Abcc4): molecular cloning, organ distribution, postnatal renal expression, and chemical inducibility. *Biochem Biophys Res Commun* **317**:46–53.
Cheung L, Flemming CL, Watt F, Masada N, Yu DM, Huynh T, Conseil G, Tivnan A, Polinsky A, Gudkov AV, et al. (2014) High-throughput screening identifies cef-401 and cef-402 as highly selective inhibitors of multidrug resistance protein 4 (MRP4). *Biochem Pharmacol* **91**:97–108.
Chi Y, Khersonsky SM, Chang YT, and Schuster VL (2006) Identification of a new class of prostaglandin transporter inhibitors and characterization of their biological effects on prostaglandin E2 transport. *J Pharmacol Exp Ther* **316**:1346–1350.
Chi Y, Pucci ML, and Schuster VL (2008) Dietary salt induces transcription of the prostaglandin transporter gene in renal collecting ducts. *Am J Physiol Renal Physiol* **295**:F765–F771.
Dey I, Lejeune M, and Chadee K (2006) Prostaglandin E2 receptor distribution and function in the gastrointestinal tract. *Br J Pharmacol* **149**:611–623.
Ferreira SH and Vane JR (1967) Prostaglandins: their disappearance from and release into the circulation. *Nature* **216**:868–873.
Gose T, Nakanishi T, Kamo S, Shimada H, Otake K, and Tamai I (2016) Prostaglandin transporter (OATP2A1/SLCO2A1) contributes to local disposition of eicosapentaenoic acid-derived PGE3. *Prostaglandins Other Lipid Mediat* **122**:10–17.
Huang SK, Wettlaufer SH, Chung J, and Peters-Golden M (2008) Prostaglandin E2 inhibits specific lung fibroblast functions via selective actions of PKA and Epac-1. *Am J Respir Cell Mol Biol* **39**:482–489.
Huang S, Wettlaufer SH, Hogaboam C, Aronoff DM, and Peters-Golden M (2007) Prostaglandin E(2) inhibits collagen expression and proliferation in patient-derived normal lung fibroblasts via E prostanoid 2 receptor and cAMP signaling. *Am J Physiol Lung Cell Mol Physiol* **292**:L405–L413.

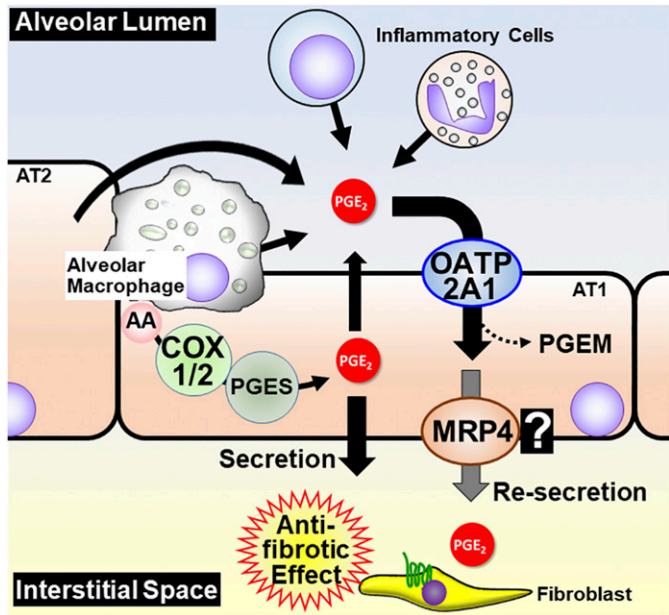


Fig. 7. Hypothesized roles of Oatp2a1 and Mrp4 in transcellular PGE₂ transport. PGE₂ secreted into alveolar lumen by alveolar epithelial cells, inflammatory cells, and alveolar macrophages can be taken up by OATP2A1 expressed at apical membranes of AT1 cells and transferred into interstitial space in cooperation with MRP4, where PGE₂ exerts an antifibrotic action. AA, arachidonic acid; PGES, prostaglandin E synthase; PGEM, prostaglandin E metabolite.

- Ikehata M, Yumoto R, Nakamura K, Nagai J, and Takano M (2008) Comparison of albumin uptake in rat alveolar type II and type I-like epithelial cells in primary culture. *Pharm Res* **25**:913–922.
- Kamo S, Nakanishi T, Aotani R, Nakamura Y, Gose T, and Tamai I (2017) Impact of FDA-approved drugs on the prostaglandin transporter OATP2A1/SLCO2A1. *J Pharm Sci* **106**:2483–2490.
- Kanai N, Lu R, Satriano JA, Bao Y, Wolkoff AW, and Schuster VL (1995) Identification and characterization of a prostaglandin transporter. *Science* **268**:866–869.
- Keerthisingam CB, Jenkins RG, Harrison NK, Hernandez-Rodriguez NA, Booth H, Laurent GJ, Hart SL, Foster ML, and McAnulty RJ (2001) Cyclooxygenase-2 deficiency results in a loss of the anti-proliferative response to transforming growth factor-beta in human fibrotic lung fibroblasts and promotes bleomycin-induced pulmonary fibrosis in mice. *Am J Pathol* **158**:1411–1422.
- Kimura H, Takeda M, Narikawa S, Enomoto A, Ichida K, and Endou H (2002) Human organic anion transporters and human organic cation transporters mediate renal transport of prostaglandins. *J Pharmacol Exp Ther* **301**:293–298.
- Kolodnick JE, Peters-Golden M, Larios J, Toews GB, Thannickal VJ, and Moore BB (2003) Prostaglandin E2 inhibits fibroblast to myofibroblast transition via E. prostanoid receptor 2 signaling and cyclic adenosine monophosphate elevation. *Am J Respir Cell Mol Biol* **29**:537–544.
- Lovgren AK, Jania LA, Hartney JM, Parsons KK, Audoly LP, Fitzgerald GA, Tilley SL, and Koller BH (2006) COX-2-derived prostacyclin protects against bleomycin-induced pulmonary fibrosis. *Am J Physiol Lung Cell Mol Physiol* **291**:L144–L156.
- Lu R, Kanai N, Bao Y, and Schuster VL (1996) Cloning, in vitro expression, and tissue distribution of a human prostaglandin transporter cDNA(hPGT). *J Clin Invest* **98**:1142–1149.
- Maher TM, Evans IC, Bottoms SE, Mercer PF, Thorley AJ, Nicholson AG, Laurent GJ, Tetley TD, Chambers RC, and McAnulty RJ (2010) Diminished prostaglandin E2 contributes to the apoptosis paradox in idiopathic pulmonary fibrosis. *Am J Respir Crit Care Med* **182**:73–82.
- Moore BB, Ballinger MN, White ES, Green ME, Herrygers AB, Wilke CA, Toews GB, and Peters-Golden M (2005) Bleomycin-induced E prostanoid receptor changes alter fibroblast responses to prostaglandin E2. *J Immunol* **174**:5644–5649.
- Nakanishi T, Hasegawa Y, Mimura R, Wakayama T, Uetoko Y, Komori H, Akanuma S, Hosoya K, and Tamai I (2015) Prostaglandin transporter (PGT/SLCO2A1) protects the lung from bleomycin-induced fibrosis. *PLoS One* **10**:e0123895.
- Nakanishi T, Ohno Y, Aotani R, Maruyama S, Shimada H, Kamo S, Oshima H, Oshima M, Schuetz JD, and Tamai I (2017) A novel role for OATP2A1/SLCO2A1 in a murine model of colon cancer. *Sci Rep* **7**:16567.
- Nomura T, Lu R, Pucci ML, and Schuster VL (2004) The two-step model of prostaglandin signal termination: in vitro reconstitution with the prostaglandin transporter and prostaglandin 15 dehydrogenase. *Mol Pharmacol* **65**:973–978.
- Oga T, Matsuoka T, Yao C, Nonomura K, Kitaoka S, Sakata D, Kita Y, Tanizawa K, Taguchi Y, Chin K, et al. (2009) Prostaglandin F(2alpha) receptor signaling facilitates bleomycin-induced pulmonary fibrosis independently of transforming growth factor-beta. *Nat Med* **15**:1426–1430.
- Pucci ML, Bao Y, Chan B, Itoh S, Lu R, Copeland NG, Gilbert DJ, Jenkins NA, and Schuster VL (1999) Cloning of mouse prostaglandin transporter PGT cDNA: species-specific substrate affinities. *Am J Physiol* **277**:R734–R741.
- Reid G, Wielinga P, Zelcer N, van der Heijden I, Kuil A, de Haas M, Wijnholds J, and Borst P (2003) The human multidrug resistance protein MRP4 functions as a prostaglandin efflux transporter and is inhibited by nonsteroidal antiinflammatory drugs. *Proc Natl Acad Sci USA* **100**:9244–9249.
- Richards RJ, Davies N, Atkins J, and Oreffo VI (1987) Isolation, biochemical characterization, and culture of lung type II cells of the rat. *Lung* **165**:143–158.
- Schuster VL (1998) Molecular mechanisms of prostaglandin transport. *Annu Rev Physiol* **60**:221–242.
- Sekine T, Watanabe N, Hosoyamada M, Kanai Y, and Endou H (1997) Expression cloning and characterization of a novel multispecific organic anion transporter. *J Biol Chem* **272**:18526–18529.
- Shimada H, Nakamura Y, Nakanishi T, and Tamai I (2015) OATP2A1/SLCO2A1-mediated prostaglandin E2 loading into intracellular acidic compartments of macrophages contributes to exocytotic secretion. *Biochem Pharmacol* **98**:629–638.
- Syeda MM, Jing X, Mirza RH, Yu H, Sellers RS, and Chi Y (2012) Prostaglandin transporter modulates wound healing in diabetes by regulating prostaglandin-induced angiogenesis. *Am J Pathol* **181**:334–346.
- Tamai I, Nezu J, Uchino H, Sai Y, Oku A, Shimane M, and Tsuji A (2000) Molecular identification and characterization of novel members of the human organic anion transporter (OATP) family. *Biochem Biophys Res Commun* **273**:251–260.
- Torky AR, Stehfest E, Viehweger K, Taege C, and Foth H (2005) Immunohistochemical detection of MRPs in human lung cells in culture. *Toxicology* **207**:437–450.
- van der Deen M, de Vries EG, Timens W, Scheper RJ, Timmer-Bosscha H, and Postma DS (2005) ATP-binding cassette (ABC) transporters in normal and pathological lung. *Respir Res* **6**:59.

Address correspondence to: Dr. Takeo Nakanishi, Faculty of Pharmaceutical Sciences, Institute of Medical, Pharmaceutical and Health Sciences, Kanazawa University, Kakuma-machi, Kanazawa 920-1192, Japan. E-mail: nakanish@p.kanazawa-u.ac.jp

Experimental evidence for re-secretion of PGE₂ across the alveolar epithelium by
OATP2A1/SLCO2A1-mediated transcellular transport

Takeo Nakanishi*, Hiroki Takashima, Yuka Uetoko, Hisakazu Komori and Ikumi Tamai

Journal of Pharmacology and Experimental Therapeutics

Supplementary Table 1

List of specific primers for rat transporter genes

Target Gene	Forward Primer (5' to 3')	Reverse Primer (3' to 5')
Oatp1a1	GTTGACCTGTGACAATGCAGC	AGCTTGATCCTCTTAGTGCTATAGG
Oatp1a4	GCCCTTTGATTGGACTTCTG	AAGGGAAAGCTGGTCAGGAT
Oatp1a5	TGGAGAACAGATCCCAGACC	TCCGATTGGCAAAGTCTTC
Oatp1b2	TGGACCAATCCTTGCTTTA	TCCTCCTGTGACCTCTTTGG
Oatp2a1	CGTCCATCTTCCTCATTTCC	GCAAGCGCATCAACAAGAAC
Oatp2b1	TTGGCAAAGGCTCAGAAGAT	ACCATGATCTGCTCCGAAAC
Mrp2	TTTTGACACAACCTCCACAGG	CAGCGATGCCAAAGAAACAC
Mrp4	CAGGGCTGCTGAATGCAATA	TTGGATTCTGGGAAGACTGAGA
Oct1	GAGGAAGGAGCCTCGTCCGAAGGT	GCAGGCCTGGCTAAACTGGTGAG
Oct2	CCATGTGTGACATTGGCGGC	AACAGCACAAAGTGCCCCAGC
Oat1	TCAGCAAAGATGGAGGTCTGG	TAAAGCGGAGGCAAGATTCTG
Cox-1	AGAACCCAATGTCCAG	GCTCCCAACCAAAATCGTAG
Cox-2	CGGACTTGCTCACTTTGTTG	TCTCTCTGCTCTGGTCAATGG
15-Pgdh	CACCATTGAGAGCATCATCTTC	CATTTGTCCAGGCTTTGTGA
Gapdh	GGGCTCTCTGCTCCTC	AGGCGTCCGATACGGC

Each primer set is used to amplify for indicated target gene.